

## ORIGINAL ARTICLE

# Sulfonated Polyacrylamide as Promising Proton Conducting Aqueous Gel Polymer Electrolyte for Tin-Air Battery

Sumathi.S,<sup>1\*</sup>Sethuprakash,<sup>2</sup>Wan Jeffrey Basirun,<sup>3,4</sup>ismail Zainol,<sup>1</sup> Sohail Ahmed,<sup>5</sup>Mehran Sookhikian<sup>6</sup>

<sup>1</sup>Department of Chemistry, Sultan Idris Education University, 35900 TanjongMalim, Perak, Malaysia.

<sup>2</sup>Department of Technical and Vocational, Sultan Idris Education University, 35900 TanjongMalim, Perak, Malaysia.

<sup>3</sup>Department of Chemistry, University Malaya, 50603 Kuala Lumpur, Malaysia.

<sup>4</sup>Institute of Nanotechnology and Catalysis (NanoCat), University Malaya, 50603 Kuala Lumpur, Malaysia.

<sup>5</sup>Department of Chemistry, Hazara University Mansehra, KPK Pakistan.

<sup>6</sup>Department of Physics, University of Malaya, Kuala Lumpur 50603, Malaysia

Tel: 016-2755464 Fax: 054585893 E mail:sumathi2311@gmail.com

### ABSTRACT

The synthesis and characterization of a new proton-conducting aqueous gel polymer electrolyte (GPE) based on sulfonated polyacrylamide (PAAm) are reported. Para-Toluenesulfonic acid monohydrate (pTSA) is used to sulfonate the PAAm in this study. This acidic GPE exhibits high ionic conductivity at room temperatures,  $9.34 \times 10^{-1} \text{ S cm}^{-1}$  with 5M of pTSA, as measured by electrochemical impedance spectroscopy. The interaction between polymer and acid in the GPE is investigated by Fourier transformed infrared (FTIR) studies. Tin-air battery, with a configuration of Sn(anode)/PAAm+pTSA/air(cathode) is fabricated at room temperature for the purpose of studying the electrochemical properties of the synthesized GPE. The battery is discharged at constant current densities of 2.5, 5, 7.5, 10, 12.5, and 15 mA  $\text{cm}^{-2}$ . The tin anode gives a discharge capacity of 440 mAh  $\text{g}^{-1}$  with an open-circuit voltage (OCV) of 1.23V at room temperature.

**Keywords:** electrochemical properties; gel polymer electrolyte; ionic conductivity; proton-conducting; sulfonated polyacrylamide

Received 15.08.2014 Accepted 20.09.2014

© 2014 AELS, INDIA

### INTRODUCTION

Proton ( $\text{H}^+$ ) conducting gel polymer electrolytes (GPE) have seen a lot of progress in the past decades per their extended applications in electrochemical cells. It is a well-established fact that proton conducting GPE can be obtained by doping polymers bearing basic units such as amide, imine, ether with strong acids, such as phosphoric acid, sulfuric acid, acetic acid, salicylic acid, or oleic acid [1-4]. Their most important characteristic is the dissociation of the acid where the proton is transferred from the acid group to the polymers with more basic groups. However, in many studies, their ionic conductivities at room temperatures are relatively low, and still unsuitable for practical applications. Conductivities of  $10^{-10} \text{ Scm}^{-1}$  to  $10^{-9} \text{ Scm}^{-1}$  has been reported for polybenzimidazole (PBI) doped with various acids, such as  $\text{H}_2\text{SO}_4$ , HCl,  $\text{HNO}_3$ ,  $\text{HClO}_4$ , and  $\text{H}_3\text{PO}_4$  [5]. In a recent study done by Isa [2], Salicylic acid-Oleic Acid were used to plasticize the poly(methyl methacrylate) GPE system. The conductivity of the GPE ( $\sim 10^{-4} \text{ Scm}^{-1}$ ) was lower than the desired conductivity (less than  $\sim 10^{-3} \text{ Scm}^{-1}$ ) for battery usage at room temperature. Poly vinyl alcohol (PVA) and sodium bromide (NaBr) solid polymer electrolyte was doped with sulfuric acid in a study conducted by Sneha [6]. The ionic conductivity of the electrolyte was increased from  $1.12 \times 10^{-6} \text{ Scm}^{-1}$  (without  $\text{H}_2\text{SO}_4$ ) to  $6 \times 10^{-4} \text{ Scm}^{-1}$  via doping with sulfuric acid. However, the XRD data revealed that sulfuric acid disrupt the semi-crystalline nature of PVA-NaBr, and render it amorphous. According to Hema, polymer electrolytes containing inorganic acids suffer from chemical degradation and mechanical integrity issues [7]. A decrease in the conductivity was observed when high concentration  $\text{H}_2\text{SO}_4$  was added into the polymer matrix [8]. The results showed a decreased hydration rate of the hydrogel, due to the degradation of the polymer matrix [8]. Thus, non-halogenated sulfonic acids are slightly less acidic, but

turned out to be interesting in the context of polymeric electrolytes. Sulfonic acids are a class of organic acids containing sulfur atom that may be part of a large aliphatic or aromatic hydrocarbon, R, with a general formula  $\text{RSO}_3\text{H}$ . The presences of hydrogen atoms render the compound acidic, with a dissociation constant of  $\sim 10^{-2}$ . The addition of trifluoromethanesulfonic acid to polymethymethacrylate (PMMA) GPE resulted in an increase of conductivity to  $\sim 10^{-3} \text{Scm}^{-1}$  [9]. The proton conductivity of p-toluenesulfonic acid doped poly (1-vinyl 1,2,4-triazole) was measured as  $8 \times 10^{-4} \text{Scm}^{-1}$  at  $150^\circ\text{C}$  and  $1.2 \times 10^{-2} \text{Scm}^{-1}$  at  $110^\circ$  [10]. The FTIR spectroscopy study proved that the proton was transferred from the acid to the triazole rings.

The present work has been undertaken to study the effect of sulfonated Polyacrylamide (PAAm) on the conductivity behavior of Polyacrylamide GPE. p-Toluenesulfonic Acid Monohydrate (pTSA) was utilized for this purpose. The variations of conductivity of the PAAm GPE as a function of acid concentration have been investigated by impedance spectroscopy. The acid-polymer interactions were studied by FTIR, and a practical application of this PAAm-pTSA GPE was studied using tin-air battery. The electrochemical properties such as open circuit voltage (OCV) and constant current discharge measurements of the tin-air battery with the PAAm-pTSA GPE were studied at room temperature.

## EXPERIMENTAL

### Preparation of PAAm-pTSA Monohydrate Gel Polymer Electrolytes

PAAm, with a molecular weight of  $M_w = 5,000,000$  as specified by the manufacturer, was procured from Polyscience, Inc., while pTSA monohydrate (>98.5%) was purchased from Sigma-Aldrich. The aqueous GPE was prepared by dissolving 1.25 g PAAm in 50 ml of distilled water. It was stirred continuously until the PAAm was fully dissolved and formed a transparent hydrogel. This was followed by the addition of 4.75 g of pTSA into the hydrogel, and it was stirred efficiently for another 24 hours in order to homogenize the GPE, with 0.5M of pTSA monohydrate. The process was repeated with 9.5 g, 19.0 g, 28.5 g, 38.0 g, 48g and 57.6g of pTSA to produce the PAAm-pTSA monohydrate GPE, with 1.0 M, 2.0 M, 3.0 M, 4.0 M, 5 M and 6 M of pTSA monohydrate, respectively.

### Characterization of PAAm-pTSA GPE

#### Electrical Impedance Spectroscopy (EIS)

The ionic conductivity measurements were carried out using the EIS method, and measured using an Autolab PGSTAT 30 potentiostat/galvanostat (Eco Chemie, B.V. Netherlands), with a frequency response analyzer (FRA) module interfaced with a computer. The samples of GPE, with different concentrations of pTSA, were analyzed at room temperature. The bulk electrolyte resistance value ( $R_b$ ), from the intercept at the real impedance axis ( $Z_R$ ) in the Nyquist plots were used to calculate the ionic conductivity ( $\sigma$ ) of the GPE with various concentrations of pTSA monohydrate. The equation below was used to calculate the ionic conductivities of the GPE samples [11].

$$\sigma = l/R_b A$$

$R_b$  = bulk resistance,  $l$  = thickness,  $A$  = Area of contact between the GPE and the electrode.

#### FTIR-Studies

The samples of PAAm-pTSA monohydrate GPE and pure PAAm were subjected to FTIR analysis to investigate the polymer-acid interactions in the GPE. The FTIR measurements were carried out on a computer-interfaced with a Perkin-Elmer System 2000 series FTIR spectrophotometer (USA), with a wavenumber range of  $4000\text{--}6000 \text{cm}^{-1}$ .

#### Discharge Characteristic of Tin-Air GPE Cell

To examine the application of the acidic GPE in an energy storage device, a tin-air cell was assembled and tested. A tin foil (99%) from Goodfellow Cambridge UK), with an active area of  $1.0 \text{cm}^2$ , was utilized as an anode. The air-cathode was made from catalytic manganese oxide  $\text{MnO}_x$  with small amount of mesoporous carbon on a Ni-mesh current collector (ECT, UK) with an area of  $0.8 \text{cm}^2$ . About 25 ml of the PAAm-pTSA monohydrate GPE with the highest conductivity was transferred into the discharge cell, with the air cathode attached to the bottom of the cell. The discharge characteristics of Tin-air cells were carried out with the Won-A-Tech WBCS 3000 (Korea Republic) battery cycler system. The (OCV) was measured for 2 hours at  $25^\circ\text{C}$ . The tin-air cells were discharged at different constant current conditions. The weight loss of tin was also measured for each discharge currents.

#### Air-Cathode of the Tin-Air Cell

##### X-ray Diffraction (XRD) and FESEM Analysis

XRD (PANalytical's Empyrean X-ray diffractometer) was used to analyze the deposits on the air-cathode after continuous discharge of the tin-air GPE cell. The surface and morphology of the air-cathode was analyzed a FEI Quanta 200F field emission scanning electron microscopy (FESEM) instrument equipped with an energy dispersive x-ray spectrum (EDX).

## RESULTS AND DISCUSSION

### FTIR of PAAm Hydrogel

The FTIR spectrum of dry PAAm is shown in Fig. 1(a). The bands at  $3393\text{ cm}^{-1}$  and  $3248\text{ cm}^{-1}$  arise from the asymmetric and symmetric stretch, respectively, of the  $\text{NH}_2$  group, which is closer to previous reports[12]. The bands at  $2930\text{ cm}^{-1}$  and  $2860\text{ cm}^{-1}$  are due to the asymmetric and symmetric stretch, respectively, of the  $\text{CH}_2$  group. The bands at  $1620\text{ cm}^{-1}$  and  $1650\text{ cm}^{-1}$  are due to the bending vibrations of the  $\text{NH}_2$  and the stretching vibrations of the  $\text{C}=\text{O}$  groups, respectively. The bands from  $1400\text{ cm}^{-1}$  to  $1200\text{ cm}^{-1}$  are also due to the  $\text{NH}_2$  group[13], while the band at  $1100\text{ cm}^{-1}$  is due to the  $\text{C}-\text{N}$  stretch[14]. These results are closer to the previous reports regarding PAAm.<sup>15</sup> Figure 1(b) shows changes of PAAm bands due to the presence of water. The broad and strong vibration around  $3000\text{--}3500\text{ cm}^{-1}$  is most probably due to the  $\text{OH}$  group in the hydrated PAAm. The  $\text{NH}_2$  bending vibration, the asymmetric and symmetric stretch of the  $\text{NH}_2$  group, and the  $\text{CH}$  asymmetric and symmetric stretch are no longer visible, due to the strong hydrogen bonding interaction between the water molecules and the PAAm. It should be noted that the  $\text{C}=\text{O}$  peak is stronger than the  $\text{NH}_2$  peaks in dry PAAm (Fig. 1(a)), but becomes weaker compared to the  $\text{OH}$  wave of around  $3400\text{ cm}^{-1}$  with the addition of water (Fig. 1(b)).

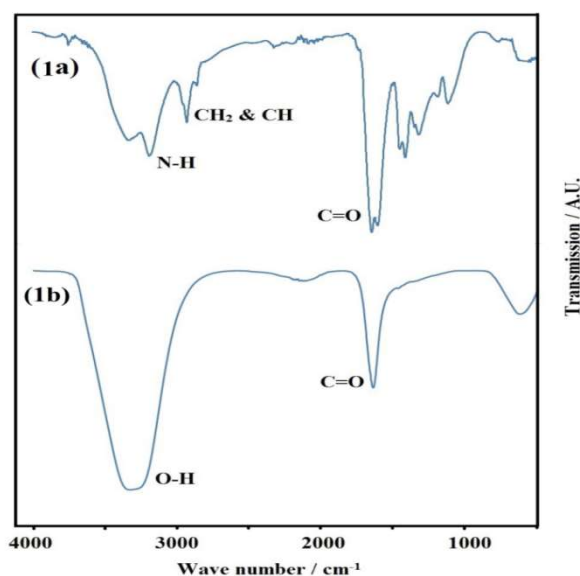


Fig 1: (a) FTIR spectra of pure PAAm; (b) PAAm with water (0M pTSA monohydrate)

### FTIR of PAA-pTSAGPE

The polymer–acid interactions of the synthesized PAAm-pTSA monohydrate GPE were also characterized by FTIR. The FTIR vibrational modes of PAAm with water (control) and PAAm with different concentrations of pTSA are shown in Fig. 2. Figure 2(a) to 2(e) show the FTIR spectra of the PAAm with the pTSA monohydrate concentrations of 1 M, 2 M, 3 M, 4 M, and 5 M, respectively. Upon the addition of the pTSA, a strong increase of the peaks at  $1185$ ,  $1125$ ,  $1035$ ,  $1013$ ,  $685$  and  $570\text{ cm}^{-1}$  (for 1 M pTSA), with the increase of the pTSA monohydrate concentration were observed. The bands for sulfonic acid and sulfonate ion showed strong vibrations between  $1150\text{--}1250\text{ cm}^{-1}$ , and medium vibrations between  $1000\text{--}1080\text{ cm}^{-1}$ [13]. The FTIR absorption range of the  $\text{O}=\text{S}=\text{O}$  asymmetric and symmetric stretching modes falls between  $1120\text{--}1230$  and  $1010\text{--}1080$ , respectively, and that of the  $\text{S}-\text{O}$  stretching lies between  $600\text{--}700\text{ cm}^{-1}$ [16,17]. Therefore, the peaks around  $1185$ ,  $1125$ ,  $1035$ ,  $1013\text{ cm}^{-1}$  are due to the asymmetric and symmetric vibrations of  $\text{O}=\text{S}=\text{O}$ , while the band of  $685$  is due to  $\text{S}-\text{O}$  stretching, which indicate the presence of sulfonic acid and sulfonate anion. The  $\text{C}-\text{S}$  stretch band is between  $705\text{--}570\text{ cm}^{-1}$ [14]. These regions seem to be the most interesting for the investigations of the PAAm-pTSA interaction, because bands originating from the groups participating in the protonation process tend to appear in these spectral ranges. In Fig 2, as the concentration of pTSA is increased, the  $\text{O}=\text{S}=\text{O}$  and  $\text{S}-\text{O}$  stretching bands appear at slightly lower frequencies with increasing intensity. For example, the peaks at  $1185$ ,  $1125$ ,  $1035$ ,  $1013\text{ cm}^{-1}$  for 1 M pTSA Fig. 2(a) were slightly shifted to  $1170$ ,  $1123$ ,  $1034$ ,  $1009\text{ cm}^{-1}$ , respectively, for 5 M pTSA (Fig 2(e)). These shifts could be due to the dissociation of the acid, which releases the  $\text{H}^+$  into the electrolytes, allowing it to participate in the hydrogen bonding with water molecules. Hydrogen

bonding interaction usually move the stretching frequencies of the participating group towards lower wave numbers, along with increased intensity and peak broadening.

The amide C=O band in the PAAm hydrogel appears at  $1637\text{ cm}^{-1}$  (Fig. 1(b)), and caused no shift upon the addition of pTSA, which suggests that the C=O was not protonated. The protonation and hydrogen bonding of the amine group leads to a peak shift to lower wave numbers[12,19]. For example, a slight shoulder peak appears at 3250, 3245 and  $3240\text{ cm}^{-1}$ , with the addition of 1 M, 2 M, 3 M, 4 M and 5 M of pTSA, respectively (Fig. 2a-2e). The notable shifts in the N-H stretching vibrations are due to the significant occurrence of protonation at the N-H group of PAAm. The association of PAAm with pTSA via protonation induced a shift of the amide band towards lower wave numbers. Fig. 3 shows the overall reaction between the pTSA and PAAm.

PAAm seems to be a very effective matrix for the formation of PAAm-pTSA GPE, as observed by FTIR. This observation is in agreement with earlier studies on PAAm based (polymer in salt) electrolytes[20,24],  $\text{H}_3\text{PO}_4$ , and  $\text{H}_2\text{SO}_4$  doped PAAm based electrolytes[19,22,23].

#### EIS and the Conductivity of PAAm-pTSA Electrolytes

EIS was used to characterize the ionic conductivity of the GPE material in this study. The Nyquist plots for PAAm with different concentrations of pTSA monohydrate at room temperatures are shown in Fig 4a-4c. The values of the bulk resistance,  $R_b$ , of the PAAm-pTSA GPE with different concentration of pTSA were determined from the intercept of the real axis,  $Z_R$  in the Nyquist plots and tabulated in Table 1. The ionic conductivity of the PAAm-pTSA monohydrate GPE for each pTSA concentration was calculated from the value of bulk resistance ( $R_b$ ) and the dimensions of the sample holder. The variation of conductivity as a function of the pTSA concentration is given in Fig 4(d).

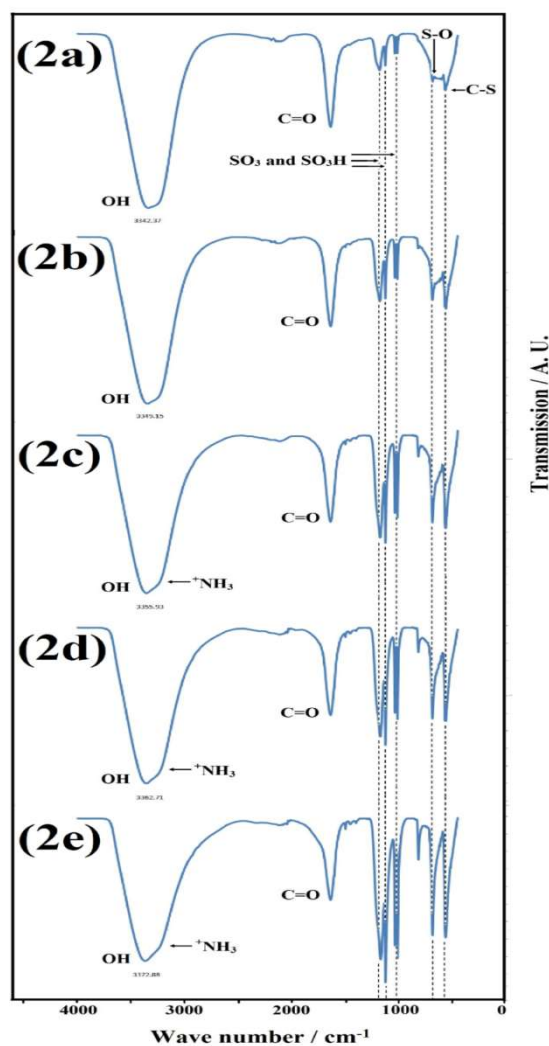


**Fig. 2:** FTIR spectra for PAAm with different concentrations of pTSA monohydrate (a) 1.0M pTSA, (b) 2.0M pTSA, (c) 3.0M pTSA (d) 4.0M pTSA (e) 5.0M pTSA

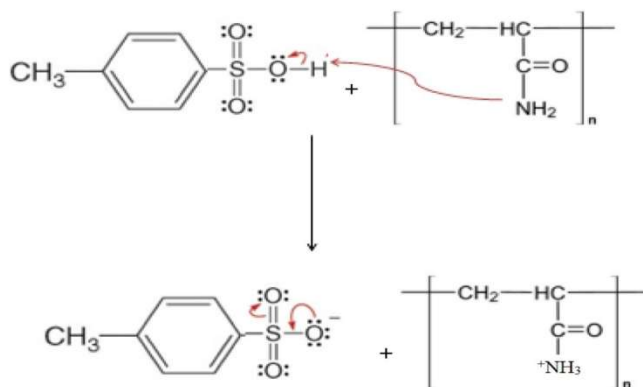


**Fig. 3: Protonation of amide group at polyacrylamide**

The ionic conductivity of the PAAm ( $\sim 10^{-3}$  S  $\text{cm}^{-1}$ ) GPE increased by nearly two orders of magnitude to  $\sim 10^{-1}$  S  $\text{cm}^{-1}$  with the addition of pTSA monohydrate. The maximum ionic conductivity of  $9.34 \times 10^{-1}$  S  $\text{cm}^{-1}$  was obtained with the addition of 5M of pTSA into polyacrylamide polymer gel. This value is slightly higher than the maximum ionic conductivity reported with methane sulfonic acid ( $7.0 \times 10^{-1}$  S  $\text{cm}^{-1}$ ) as an additive to PAAm polymer gel electrolyte[22]. Literature reports on PAAm hydrogel with strong inorganic acids, such as  $\text{H}_3\text{PO}_3$  or  $\text{H}_2\text{SO}_4$  as additives result in ionic conductivities between  $10^{-3}$  and  $10^{-2}$  S  $\text{cm}^{-1}$ [23,24,25]. In the present study, pTSA monohydrate as an additive to PAAm results in higher ionic conductivity values between the ranges of  $\sim 10^{-1}$  S  $\text{cm}^{-1}$ .

The pTSA ionizes and releases hydrogen ions ( $\text{H}^+$ ) into the polymer matrix. The ionization of pTSA is influenced by the p-toluenesulfonate ion stability, due to the resonance effect. Figure 5 shows the three resonance structures of the p-toluenesulfonate ion. The resonance effect stabilizes the negative charge on the p-toluenesulfonate ion by the delocalization of charges on the oxygen atoms[26]. Increased stabilization of the anion can be achieved via larger areas of charge delocalization in the benzene ring[27]. The  $\text{H}^+$  released from the pTSA migrates to the PAAm through the free volume of polymer matrices. The available mobile hydrogen ions ( $\text{H}^+$ ) from the ionization of the pTSA are the main factor for the increases in ionic conductivity of the GPE with the increase of the pTSA concentration.

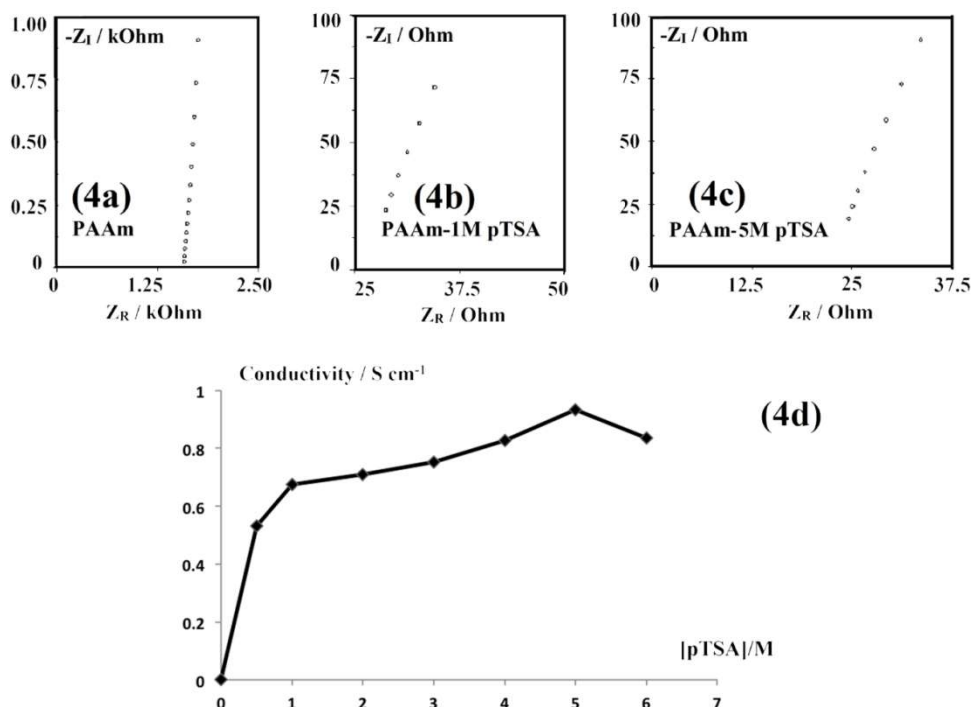


**Fig.4:** The impedance plot of PAAm/xMpTSA monohydrate GPE (a) PAAm with water (b) PAAm with 1M pTSA monohydrate (c) PAAm with 5M pTSA monohydrate (d) Variation of conductivity of PAAm-pTSA monohydrate GPE as the function of pTSA monohydrate concentration.

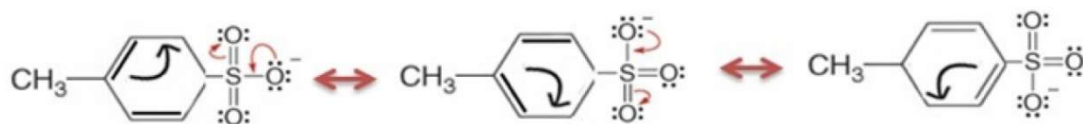


Fig.5: Resonance structures of sulfonate anion.

Table 1: The Values of the Bulk Resistance,  $R_b$ , of the PAAm-pTSAGPE with Different Concentration of pTSA

| Concentration of pTSA (M) | Bulk resistance / $R_b$ |
|---------------------------|-------------------------|
| 0                         | 17900                   |
| 0.5                       | 32.92                   |
| 1.0                       | 26.00                   |
| 2.0                       | 24.70                   |
| 3.0                       | 23.30                   |
| 4.0                       | 21.00                   |
| 5.0                       | 18.80                   |
| 6.0                       | 20.95                   |

#### Discharge Behavior of Tin-Air Cell with PAA-pTSAMonohydrate GPE

Tin-air cell based on PAAm-pTSA monohydrate GPE was evaluated for their constant current discharge performance at room temperatures. The PAAm-5M pTSAGPE, with the highest conductivity value of  $9.34 \times 10^{-1} \text{ S cm}^{-1}$ , was used to assemble the tin-air cells. The OCV increases to up to 1.23 V, and remains practically constant without any significant drops (Fig. 6).

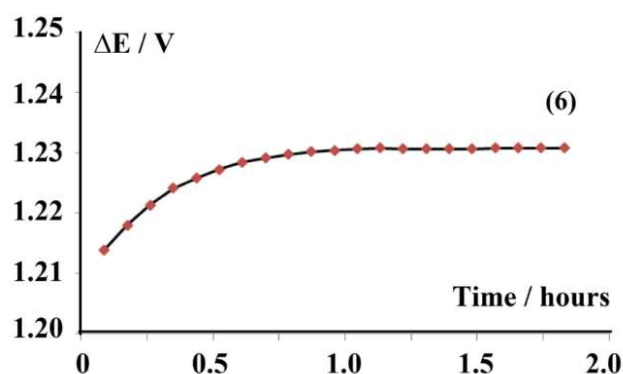
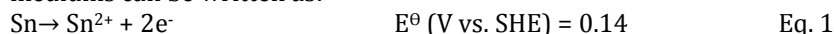


Fig.6: OCV of tin-air cell with/PAAm-5M pTSA GPE for 2 hours of at room temperature.

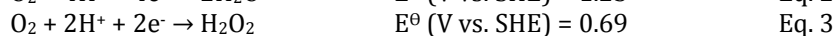
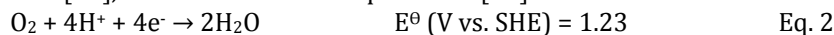
The discharge curves of the tin-air GPE cell obtained at different discharge current rates are given in Fig 7. It can be observed that the discharge time of the cell decreases with the increase of the discharge current. The discharge capacity was calculated from the specific capacity of anode tin metal. The capacity of the tin-air cell was determined only from the amount of the active tin metal in the anode, since the capacity of the air cathode is infinitely high, due to the inexhaustible supply of oxygen in the atmosphere[28].

The tin anode of the cell with PAAm-4M pTSA polymer electrolyte results in an average capacity of  $440 \text{ mAh g}^{-1}$ . The current efficiencies were calculated from the Faraday equation,  $It = mnF$ , and from the weight loss of the tin anode and the discharge profiles in Fig. 7(a). It was found that the current efficiencies were close to 100% for an  $n$  value of 2. This suggests that the Sn was oxidized to  $\text{Sn}^{2+}$ , and no

further oxidation to  $\text{Sn}^{4+}$  took place during the cell discharge. The oxidation of Sn to  $\text{Sn}^{2+}$  in acidic mediums can be written as:



The oxygen reduction reaction on the air cathode in acidic solutions depends on the concentration of acid used[29], and has the standard potentials[30]:



Eq. 2 occurs at higher concentrations of acid. Thus, the most probable reaction at the air cathode in PAAm-5M pTSA is Eq. 2, as the combination of Eq. 1 and Eq. 2 is closer to the OCV value. The highest power density shown by the cell with PAAm-5M pTSA as the GPE is  $3.19 \text{ mW cm}^{-2}$ , as shown in Fig. 7(b).

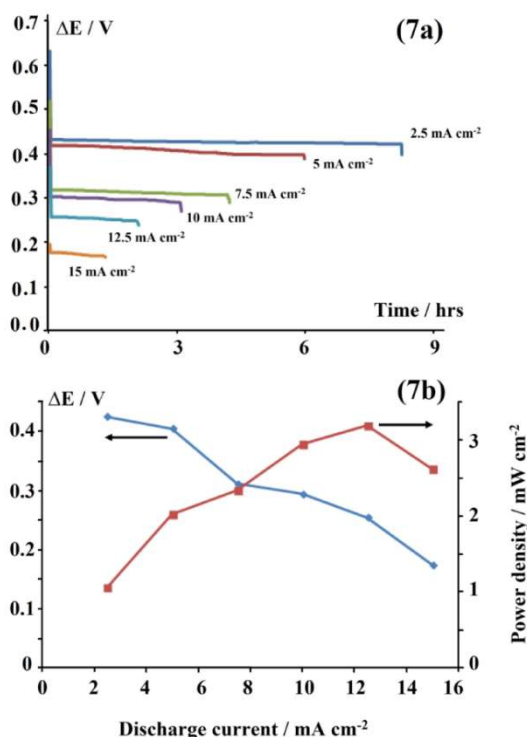


**Fig 7: (a)** The discharge curve of tin-air cells with different discharge current (b) Power density at different discharge current

### XRD, FESEM and EDX on Air Cathode

After a continuous constant current discharge of the cell, the surface of the air-cathode changed from black to a mixture of white spots with black background. XRD analysis was performed on the air cathode after discharge to investigate the deposits on the air

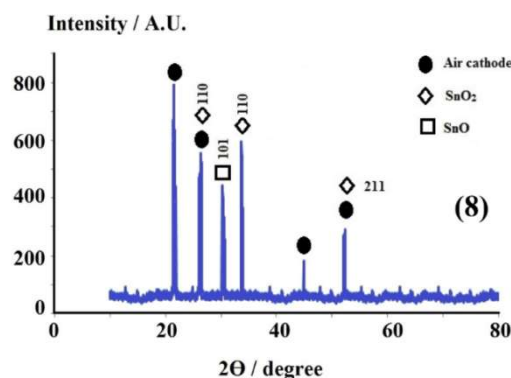


**Fig. 8: XRD of air-cathode after complete discharge**

cathode surface. Fig. 8 shows the XRD of the air cathode after continuous constant current discharge of the tin-air GPE cell. The  $2\theta$  degree for  $\text{SnO}_2$  occurs at  $26.45^\circ$ ,  $33.65^\circ$ , and  $51.62^\circ$ , while the intensity for  $\text{SnO}$  occurs at  $30.11^\circ$ . The XRD results indicates that the deposits are tetragonal  $\text{SnO}_2$ , with cell parameters of  $a=0.472\text{nm}$  and  $c=0.317\text{nm}$ . These parameters agree with the standard data (ICDD-PDF41-1445). The results closely match the standard XRD data files of  $\text{SnO}$  (PDF number 00-006-0395 ICOD) and  $\text{SnO}_2$  (PDF number 01-072-1147 ICOD).

Fig. 9 shows the FESEM micrographs and the EDX of the air-cathode after continuous constant current discharge of the tin-air GPE cell. Fig. 9(a) shows that the formation of tin oxides occurs largely on the surface of the Ni mesh current collector, while Fig. 9(d) is the air cathode surface before it is discharged, placed there for comparison purposes. Figs. 9(b) and 9(c) shows a larger magnification of the selected area in Fig. 9a, which reveals a rod-like structure of the tin oxides. The EDX spectrum in Fig. 9(e) was also taken for the air-cathode after discharge, and shows that the main elements of the air-cathode electrode are C, O, Ni, S and Sn. The EDX spectrum also indicates the presence of Sn and O at the surface of the air-cathode.

From the XRD result in Fig. 8, the deposition of  $\text{SnO}$  and  $\text{SnO}_2$  on the air cathode from continuous constant current discharge of the tin-air GPE cell can be described by the following reactions:

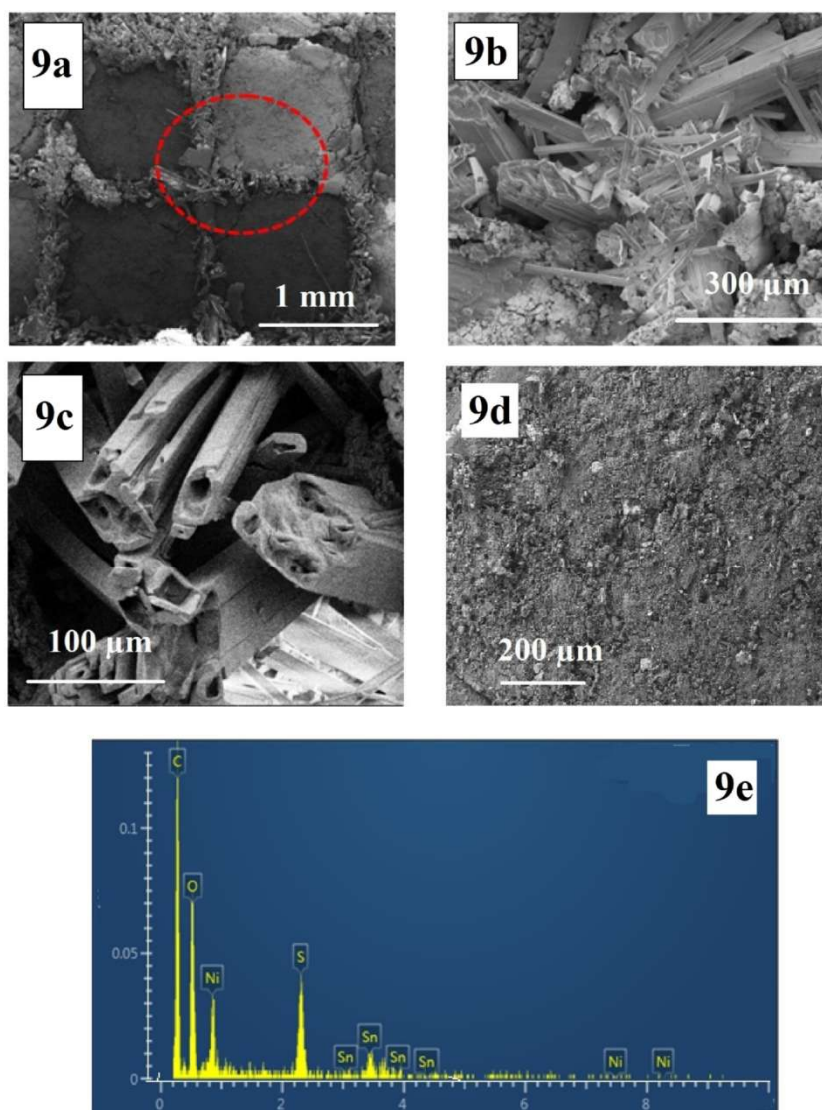


Fig.9: FESEM and EDX of air-cathode surface after complete discharge; (a) Formation of the tin oxide on the surface of the Ni mesh current collector (b) Rod-like structure of tin-oxide (c) Larger magnification of the formation of tin oxides (d) Air cathode surface before discharge (e) EDX spectrum

## CONCLUSIONS

This work describes the investigative efforts in developing a new proton conducting gel polymer electrolyte based on PAAm-pTSA monohydrate. The effect of p-toluenesulfonic acid concentration on the ionic conductivity of the GPE was investigated by EIS. The maximum ionic conductivity of the GPE was  $9.34 \times 10^{-1} \text{ S cm}^{-1}$  with the addition of 5 M pTSA monohydrate. The specific interactions between the pTSA monohydrate, PAAm, and water constituents into the GPE were confirmed by FTIR analysis. The protonation occurred at the amide group of PAAm. Tin-air GPE cells, with tin as the anode and  $\text{MnO}_2$  as the cathode, and with PAAm and 5 M pTSA monohydrate as the GPE, was successfully assembled and characterized. The cell provided an OCV of 1.23V and specific discharge capacity of  $440 \text{ mAh g}^{-1}$ . Due to its good inherent electrochemical properties and easy access, the PAAm-pTSA GPE shows promise in tin-air battery application.

## ACKNOWLEDGEMENTS

The authors would like to thank University Malaya and Ministry of Higher Education, for providing financial assistance with grant number FP033 2013A and RG181-12SUS for this work.

## REFERENCES

1. Bozkurt A, Meyer WH, Wegner G(2003).PAA/imidazol-based proton conducting polymer electrolytes. *J.Power Sources*. 123(2):126-131.
2. M. Isa(2012). Poly (Methyl Methacrylate)-Salicylic Acid-Oleic Acid Plasticized Gel Electrolyte System: Electrical and Ionic Transport Study. *Res. J.Phys*.6(2): 50-58.
3. He R, Li Q, Xiao G, and Bjerrum NJ(2003). Proton conductivity of phosphoric acid doped polybenzimidazole and its composites with inorganic proton conductors. *J.Membr.Sci*.226(1):169-184.
4. Sekhon, Singh HP(2004). Polymer gel electrolytes containing acetic acid and chloro substituted mono, di and trichloroacetic acids with PMMA and pVdF-HFP as gelling polymer.*Solid State Ion*.175:545-548.
5. Xing B, and Savadogo O. (1999). The effect of acid doping on the conductivity of polybenzimidazole (PBI). *J New Mat Elect Syst*.2: 95-102.
6. Sheha, E., & El-Mansy, M. K. (2008). A high voltage magnesium battery based on  $\text{H}_2\text{SO}_4$  -doped (PVA) /( $\text{NaBr}$ ) Solid polymer electrolyte. *Journal of Power Sources*.185(2): 1509-1513.
7. Hema M, Selvasakerpandian S, Sakunthala A, Arunkumar D, and Nithya H. (2008). Structural,vibrational and electrical characterization of PVA- $\text{NH}_4\text{Br}$  polymer electrolyte system. *Physica B*. 403:2740-2747.
8. MohamedM (2012)Characterization of Polyvinyl acetate/Epoxy Blend Foam. *J ChemEng Pro Tech*.34:121-125.
9. KumarR,SekhonS (2013). Conductivity, FTIR studies, and thermal behavior of PMMA-based proton conducting polymer gel electrolytes containing triflic acid, *Ionics*. 1-9.
10. Özden, Çelik SMU,Bozkurt A (2010). Polymer electrolyte membranes based on p-toluenesulfonic acid doped poly (1-vinyl-1, 2, 4-triazole): Synthesis, thermal and proton conductivity propertiesJ *Polym Sci Pol Phys*. 48:1016-1021.
11. Reddy ALM, ShaijumonMM,GowdaSR,Ajayan PM (2009). Coaxial  $\text{MnO}_2$ /carbon nanotube array electrodes for high-performance lithium batteries, *Nano Lett*.9: 1002-1006.
12. Yih, S.W.;Hai, C.C.;Jyh, C.J.; Sheng, H.L.; Yuan, T.L.;Huan, C.C (1998). Structures and Isomeric Transitions of  $\text{NH}_4^+(\text{H}_2\text{O})_{3-6}$ : From Single to Double Rings, *J. Am. Chem. Soc*.120:8777-8788.
13. Infrared Correlation Charts. In *CRC Handbook of Chemistry and Physics, 90th Edition (CD-ROM Version 2010)*. Edited by Lide DR. Boca Raton FL: CRC Press/Taylor and Francis 1461.
14. Coates, J (2000).Interpretation of Infrared Spectra, a Practical Approach. In *Encyclopedia of Analytical Chemistry*,Wiley.10815-10837.
15. Deng Y, Dixon JB, White GN, Loeppert RH, Juo AS. (2006). Bonding between polyacrylamide and smectite. *Colloids and Surfaces A: Colloid Surf. A Physicochem. Eng. Asp*. 281:82-91.
16. Meng F, Zhang B, Li L, and Zang B. (2003). Liquid-crystalline elastomers produced by chemical crosslinking agents containing sulfonic acid groups. *Polymer*. 44: 3935-3943.
17. Basavaiah K, AVPrasadaRao(2012). Preparation and characterization of pTSA doped tetraaniline nanorods via Micellar - Assisted Method.*J. Chem*. 9:1175-1180.
18. Wanchoo RK, and Sharma PK. (2003). Viscometric study on the compatibility of some water-soluble polymer-polymer mixtures. *Eur. Polym. J*.39 (7):1481-1490.
19. Wiczeorek W,Stevens (1997).Proton transport in polyacrylamide based hydrogel doped with  $\text{H}_3\text{PO}_4$  or  $\text{H}_2\text{SO}_4$ .*Polymer*.38:2057-2065.
20. Zalewska A, Pruszczykl, SułekE, Wiczeorek W (2003).New poly(acrylamide) based polymer in salt electrolytes: preparation and spectroscopic characterization.*Solid State Ion*. 157: 233-239.
21. Rodrigues PC, Cantão MP, Janissek P, Scarpa PC, Mathias AL, Ramos LP, and Gomes, MA(2002). Polyaniline/lignin blends: FTIR, MEV and electrochemical characterization. *Eur. Polym. J*. 38:2213-2217.
22. Sumathi S, Sethuprakash V, Basirun W J, Zainol I, and Sookhakistan M. (2014). Polyacrylamide-methanesulfonic acid gel polymer electrolytes for tin-air battery.*M.J Sol.GelSci Techno*.69:480-487.
23. Wiczeorek, W.; Florjanczyk, Z.;Stevens, Proton conducting polymer gels based on a polyacrylamide matrix *J. Electrochim. Acta*.**1995**,40,2327-2330.

24. Stevens J, Wieczorek W, Raducha D, Jeffrey (1997). Proton Conducting Gel/H<sub>3</sub>PO<sub>4</sub> Electrolytes K. Solid State Ion. 97:347-358.
25. Song W, Wang Y, and Deng H (2004). Ion-conducting polymer gels of polyacrylamide embedded with K<sub>2</sub>CO<sub>3</sub>. J. Appl. Polym. Sci. 92: 2076-2081.
26. Stadniy IA, Konovalova VV, Samchenko YM, Pobigay GA, Burban AF, and Ulberg ZR (2011). Development of hydrogel polyelectrolyte membranes with fixed sulpho-groups via radical copolymerization of acrylic monomers. Mater Sci Appl. 2:270-275.
27. Chwaleba D, Ilczyszyn MM, Ilczyszyn M, and Ciunik Z. (2007). Glycine–methanesulfonic acid (1: 1) and glycine–p-toluenesulfonic acid (1: 1) crystals: Comparison of structures, hydrogen bonds, and vibrations. J. Mol. Struct. 831:119-134.
28. Kaisheva, A (2005). Proceedings of the International Workshop: Portable and Emergency Energy Sources—from Materials to Systems, Primorsko, Bulgaria.
29. Khomenko VG, Barsukov V Z, and Katashinskii AS (2005). The catalytic activity of conducting polymers toward oxygen reduction. Electrochim. Acta. 50:1675–1683.
30. Lide, D.R.; Boca, Raton. F. L. Electrochemical Series, In *CRC Handbook of Chemistry and Physics, 90th Edition (CD-ROM)*. CRC Press/Taylor and Francis. 2010, 1218-1219.

**CITE THIS ARTICLE**

Sumathi.S, Sethuprakash, Wan Jeffrey B, Ismail Zainol, Sohail A, Mehran S. Sulfonated Polyacrylamide as Promising Proton Conducting Aqueous Gel Polymer Electrolyte for Tin-Air Battery. Res J. Chem. Env. Sci. Vol 2 [5] October 2014. 38-47